Tyrosine Kinase Inhibitors. 11. Soluble Analogues of Pyrrolo- and Pyrazoloquinazolines as Epidermal Growth Factor Receptor Inhibitors: Synthesis, Biological Evaluation, and Modeling of the Mode of Binding

Brian D. Palmer,[†] Susanne Trumpp-Kallmeyer,[‡,§] David W. Fry,[‡] James M. Nelson,[‡] H. D. Hollis Showalter,[‡] and William A. Denny*[,†]

Cancer Society Research Laboratory, Faculty of Medicine and Health Science, The University of Auckland School of Medicine, Private Bag 92019, Auckland 1000, New Zealand, and Parke-Davis Pharmaceutical Research, Division of Warner-Lambert Company, 2800 Plymouth Road, Ann Arbor, Michigan 48106-1047

Received November 12, 1996[⊗]

A new route to N-1-substituted pyrazolo- and pyrroloquinazolines has been developed from the known quinazolones **19** and **23**, via conversion to the corresponding thiones, S-methylation to the thioethers, N-1-alkylation, and coupling with 3-bromoaniline. C-3-Substituted pyrroloquinazolines were prepared by Mannich base chemistry. A series of compounds bearing solubilizing side chains at these positions has been prepared and evaluated for inhibition of the tyrosine kinase activity of the isolated epidermal growth factor receptor (EGFR) and of its autophosphorylation in EGF-stimulated A431 cells. Several analogues, particularly C-3-substituted pyrroloquinazolines, retained high potency in both assays. A model for the binding of the general class of 4-anilinoquinazolines to the EGFR was constructed from structural information (particularly for the catalytic subunit of the cAMP-dependent protein kinase) and structure−activity relationships (SAR) in the series. In this model, the pyrrole ring in pyrroloquinazolines (and the 6- and 7-positions of quinazoline and related pyridopyrimidine inhibitors) occupies the entrance of the ATP binding pocket of the enzyme, with the pyrrole nitrogen located at the bottom of the cleft and the pyrrole C-3 position pointing toward a pocket corresponding to the ribose binding site of ATP. This allows considerable bulk tolerance for C-3 substituents and lesser but still significant bulk tolerance for N-1 substituents. The observed high selectivity of these compounds for binding to EGFR over other similar tyrosine kinases is attributed to the 4-anilino ring binding in an adjacent hydrophobic pocket which has an amino acid composition unique to the EGFR. The SAR seen for inhibition of the isolated enzyme by the pyrazolo- and pyrroloquinazolines discussed here is fully consistent with this binding model. For the N-1-substituted compounds, inhibition of autophosphorylation in A431 cells correlates well with inhibition of the isolated enzyme, as seen previously for related pyridopyrimidines. However, the C-3-substituted pyrroloquinazolines show unexpectedly high potencies in the autophosphorylation assay, making them of particular interest.

The epidermal growth factor receptor (EGFR) is known to be overexpressed in a large percentage of clinical cancers of various types[1−3] and to be associated with poor prognosis.[4,5] Compounds which inhibit the ability of EGFR to transmit a phosphorylation signal following binding of its cognate ligand EGF are therefore of potential interest as anticancer drugs, and this is an active field of drug development. A number of reports[6−16] have shown that the broad class of 4-anilinoquinazolines are potent and highly selective inhibitors of EGFR phosphorylation, resulting from competitive binding at the ATP site.[6] We have previously demonstrated structure−activity relationships (SAR) for compounds related to the parent compound **1**, showing the utility of small lipophilic groups in the 3′-position[7] and of electron-donating substituents in the 6- or 7-position.[9] In a later paper,[10] we showed that linear tricyclic derivatives which incorporated electron-donating amino substituents into a fused 5- or 6-membered aromatic ring were also potent inhibitors. Thus the pyrazolo- and pyrroloquinazoline compounds **2a** and **3a** both showed IC_{50} values of 0.44 nM for inhibition of the isolated enzyme.[10] However, the poor aqueous solubility of these compounds is a major drawback to their further development.

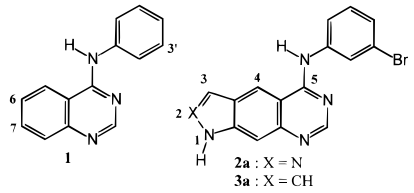

In the present paper we discuss a possible binding mode for these inhibitors on the EGFR enzyme. This uses a molecular model of the EGFR TK constructed from the refined structure of the catalytic subunit of the cAMP-dependent protein kinase[17] and structure−activity relationships for competitive inhibition by a series of quinazolines, pyrido[*d*]pyrimidines, and fused tricyclic quinazolines.[8−11,16] Partly on the basis of this model, several more soluble analogues of both the **2** and **3** tricyclic series (**2b**−**d**,**f**,**h**, **3b**−**h**, and **4**−**9**) were prepared and evaluated.

Chemistry

The acetic acid derivatives **2h** and **3h** were prepared by direct alkylation of the known[10] parent heterocycles

[†] The University of Auckland School of Medicine.
[‡] Parke-Davis Pharmaceutical Research.
[§] Address correspondence regarding molecular modeling to this author.
[⊗] Abstract published in *Advance ACS Abstracts,* April 1, 1997.

S0022-2623(96)00789-3 CCC: $14.00

Scheme 1[a]

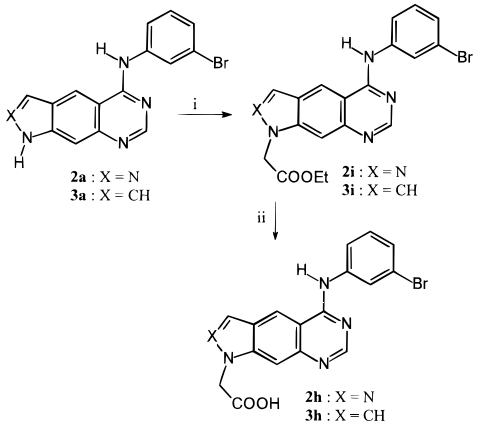

[a] (i) NaH/20 °C/5 min, then $BrCH_2COOEt$/20 °C/1.5 h; (ii) 2 N NaOH/MeOH/30 min.

Scheme 2[a]

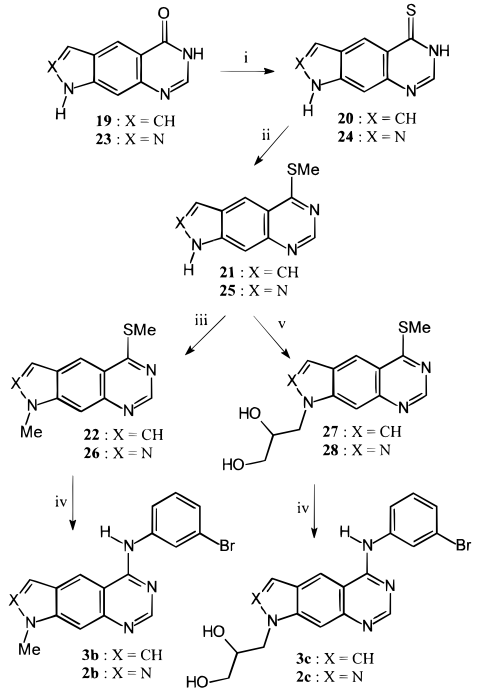

[a] (i) P_2S_5/pyridine/reflux/18 h; (ii) MeI/1 N NaOH/20 °C/2 h; (iii) NaH/20 °C/5 min, then MeI/20 °C/30 min; (iv) 3-bromoaniline/concentrated HCl/120 °C/4 h; (v) NaH/20 °C/5 min, then $ClCH_2CH(OH)CH_2OH$/45 °C/30 min.

2a and **3a**, using ethyl bromoacetate on the 1-sodio derivatives followed by base hydrolysis of the resulting esters (Scheme 1). Attempts to introduce 1-methyl and 1-(dihydroxypropyl) substituents in an analogous manner were unsuccessful, due primarily to the formation of inseparable mixtures of products resulting from alkylation in the anilinoquinazoline ring in addition to the desired N-1 position. The required compounds were eventually synthesized as shown in Scheme 2. The known[10,15] quinazolones **19** and **23** were converted into the corresponding thiones **20** and **24**, which were methylated to form the thioethers **21** and **25** in good yield. Alkylation of the thioethers with methyl iodide or 1-chloropropane-2,3-diol proceeded cleanly at the N-1 position, and the resulting products (**22** and **26**−**28**) were reacted with 3-bromoaniline at 120 °C to give the desired 5-anilino derivatives. This also proved a significantly superior route to the parent compounds **2a** and **3a**. The previously reported[10] route to these compounds via the 4-chloroquinazolines gave much lower yields, due largely to the very low solubility of **19** and **23**.

Scheme 3[a]

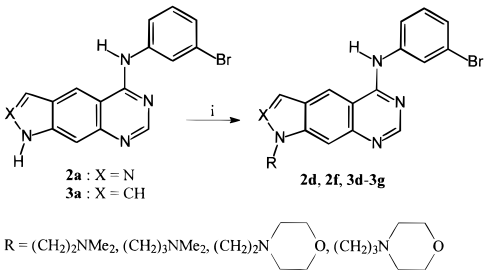

[a] (i) RCl·HCl/$CsCO_3$/4A molecular sieves/Me_2CO/reflux/24−48 h.

Scheme 4[a]

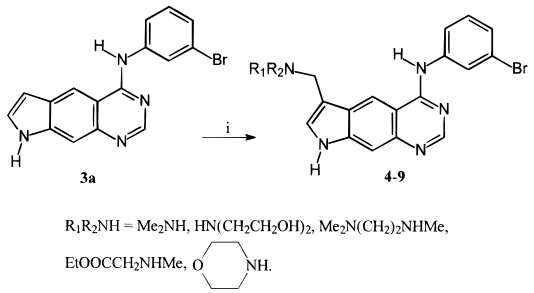

[a] (i) R_1R_2NH/HCHO/AcOH/50 °C/1−3 h.

Preparation of the tricycles bearing amino side chain substituents at N-1 was best achieved (albeit in only moderate yields) by treating the parent heterocycle with the hydrochloride salt of the appropriate chloroalkylamine in the presence of cesium carbonate and powdered 4A molecular sieves (Scheme 3). Finally, introduction of solubilizing substituents at the 3-position of the pyrroloquinazoline was achieved by a Mannich reaction between the parent pyrroloquinazoline **3a**, formaldehyde, and the appropriate secondary amine, in acetic acid at 50 °C (Scheme 4). Although quite stable at room temperature, these 3-substituted products decomposed at temperatures above ca. 130 °C, regenerating the starting tricycle in a reverse Mannich reaction.

Proposed Model for 4-(Phenylamino)-quinazoline Binding to EGFR

Structure−Activity Relationship Studies. Some information identifying a possible binding mode on the enzyme comes from the SAR of a large number of 4-(phenylamino)quinazolines for inhibition of the phosphorylation by EGFR of a fragment of phospholipase Cγ1 (Table 1). The core 4-(phenylamino)quinazoline pharmacophore **1** has an IC_{50} of 346 nM in this assay, with a clear benefit resulting from small lipophilic electron-withdrawing groups at the 3-position of the anilino moiety.[8] Thus, substitution of **1** with 3′-Br to give **10** increases inhibitory potency more than 10-fold (IC_{50} 27 nM). However, substitution of the anilino side chain at other positions, or with larger groups, greatly reduces activity, suggesting limited bulk tolerance.[16] The requirement for the quinazoline structure was established by studying alterations in the nitrogen substitution pattern within the bicyclic ring system.[8]

Table 1. Structure−Activity Relationships for Inhibition of EGFR by 4-(Phenylamino)quinazolines

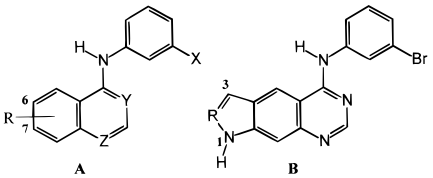

no.	formula	R	X	Y	Z	IC_{50} (nM)[a]	ref
1	A	H	H	N	N	346	8
10	A	H	Br	N	N	27	8
11	A	H	Br	N	C	>100000	8
12	A	H	Br	C	N	5500	8
13	A	6,7-diOEt	Br	N	N	0.006	9
14	A	6,7-diOMe	Br	N	N	0.025	9
15	A	2-Me	Br	N	N	>10000	9
16	A	8-OMe	Br	N	N	>10000	9
2a	B	N				0.44	10
3a	B	CH				0.44	10

[a] IC_{50}, concentration of drug (nM) to inhibit the phosphorylation of a 14-residue fragment of phospholipase Cγ1; see references.

Substitution of the N-1 in **1** by carbon to give **11** resulted in a >3700-fold loss of activity, whereas similar substitution of N-3 (to give **12**) produced a 200-fold loss. This indicates the importance of both nitrogens in the interaction with the enzyme (potentially as H-bond acceptors). Substitution of C-2 in the quinazoline ring system of **1,** even with small substituents such as Me (e.g., **15**), abolishes activity,[9] while substituents at C-8 (e.g., **16**) are not favorable.[8] This face of the pharmacophore therefore also appears to bind to an area of restricted size. In sharp contrast, steric bulk can be readily tolerated at the 6- and 7- positions, as exemplified by the 4-(3-bromoanilino)-6,7-dialkoxyquinazolines. The diethoxy compound **13** shows similar potency (IC_{50} 0.006 nM) to the corresponding dimethoxy analogue **14**.[9] Moreover, as noted above, a third ring can be fused to the bicyclic quinazoline ring system without loss of binding affinity (e.g., **2a** and **3a** both have IC_{50}s of 0.44 nM).[10] Generally, where comparisons have been made, the pyrido[*d*]pyrimidines also show similar SAR to the quinazolines.[11] In the parent compounds, aza substitution in the ring at the 5−7-positions has little effect, but at the 8-position, this substitution is strongly detrimental.

Structural Data from Other Protein Kinases. The ATP binding site is a common feature of the entire PK family and is defined by two β-sheets that form a cleft between the N- and C-terminal lobes. In the 3D model of EGFR TK constructed from the refined structure of the catalytic subunit of the cAMP-dependent protein kinase,[17] the adenine base is anchored by a bidentate donor−acceptor hydrogen-bonding motif. The hydrogen bonds between the N-6 hydrogen and the backbone carbonyl of Gln-767 and between N-1 and the backbone amide of Met-769 fix the purine onto the extended coil stretch that connects the N-terminal lobe with the C-terminal lobe of the enzyme. A third hydrogen bond between N-7 and the hydroxyl group of Thr-830 located on strand 8 preceding the activation loop may be less important because it is not conserved in all protein kinases.

Nonpolar interactions with one face of the purine ring occur with Val-702 on strand 3 and Ala-719 and Leu-768 which are part of the conserved glycine-rich flap. Nonpolar interactions from the opposite face come from Leu-820 on strand 7 and Thr-830 on strand 8. The ribose and the triphosphate moieties extend toward the opening of the cleft where the phosphate transfer occurs. The ribose 2′-OH can form a hydrogen bond with Cys-773, either directly (as in cAMP kinase) or indirectly through water (as in casein kinase). The same binding mode has been observed in several recently published protein kinase structures in agreement with the high degree of sequence conservation present in the catalytic core of protein kinases.[18−21] Despite the high degree of homology, there are some significant amino acid differences in the ATP binding site of EGFR TK compared to other tyrosine kinases, which presumably account for the high selectivity of this class of compounds for the EGFR TK. The entrance of the binding pocket, which includes the Cys-773 residue, is considerably more hydrophobic than in PDGFR (Asp), FGFR (Asn), or c-src (Ser). An investigation of the ATP binding pocket for the EGFR TK shows three additional sulfur-containing amino acid residues (Cys-751, Met-769, and Met-742). In particular, the Cys-751 residue on strand 4 is only present in EGFR TK and is part of a hydrophobic pocket adjacent to the ATP binding pocket. This pocket is present in the other tyrosine kinases as well but is more shallow due to the exchange of Cys-751 for Val or Ile.

The ATP competitive inhibitor isopentyladenine (**17**) has been cocrystallized with the similar enzyme CDK2 and forms a homologous bidentate hydrogen bond with the backbone of the corresponding amino acid residues on the extended coil stretch. The crystal structure of CDK2 complexed with the inhibitor olomucine (**18**) also

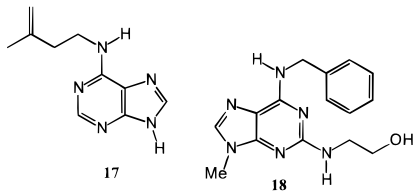

shows a bidentate hydrogen bond between the inhibitor and the extended coil stretch, although one of the hydrogen bonds is formed with the backbone of a different amino acid residue, located closer to the entrance of the ATP binding pocket.[21] These structural data also suggest that hydrogen bonding is essential for inhibitor binding, although the same amino acids on the extended coil stretch are not necessarily involved. The above hydrogen bond donor−acceptor is not present in the 4-(phenylamino)quinazolines. Nevertheless, the SAR studies (discussed above) indicate an essential role for the quinazoline N-1 and an important role for N-3, suggesting that both nitrogens might act as hydrogen bond acceptors. The 3D model of the EGFR TK suggests that these hydrogen bonds are formed with amino acid residues from the extended coil stretch at the bottom of the ATP binding site cleft.

Results and Discussion

The structures and physicochemical properties of the new tricyclic derivatives prepared are given in Table 2. All the analogues were evaluated for their ability to inhibit tyrosine phosphorylation of a random copolymer of tyrosine and glutamic acid (Sigma) by EGF-stimulated full-length EGFR enzyme isolated from A431 cells.[6] Full dose−response curves were determined for

Table 2. Structural and Biological Properties of Soluble Substituted 5-[(3-Bromophenyl)amino]pyrrolo[3,2-*g*]quinazolines and -pyrazolo[4,3-*g*]quinazolines

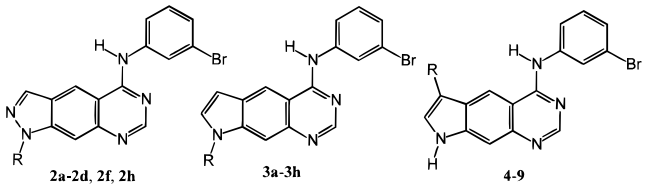

				IC_{50} (nM)[a]	
no.	R	mp or ref	sol (mM)	EGFR	autophos
		Pyrazolo Series			
2a	H	ref 10	0.11	0.44	20
2b	Me	227−229	0.33	0.37	13
2c	$CH_2CH(OH)CH_2OH$	261	0.10	12	318
2d	$(CH_2)_2NMe_2$[b]	262−264	36	40	262
2f	$(CH_2)_2$Nmorpholide[c]	216−220		3.7	192
2h	CH_2COOH	252 dec	0.26	53	1196
		Pyrrolo N-Substituted Series			
3a	H	ref 10	1.5	0.44	22
3b	Me	178−180	0.49	0.80	22
3c	$CH_2CH(OH)CH_2OH$	184−187	9.7	1.6	49
3d	$(CH_2)_2NMe_2$	150−152		41	145
3e	$(CH_2)_3NMe_2$	171−172	11	21	230
3f	$(CH_2)_2$Nmorpholide	114−116	2.5	3.7	16
3g	$(CH_2)_3$Nmorpholide	123−126	2.4	8.8	77
3h	CH_2COOH	>170 dec	11	5.1	1780
		Pyrrolo 3-Substituted Series			
4	$CH_2N(CH_2CH_2OH)_2$	240−245 dec		3.5	135
5	CH_2NMe_2	220 dec	20	2.6	9.7
6	CH_2Nmorpholide	229 dec	11	4.8	9.6
7	$CH_2N(Me)(CH_2)_2NMe_2$	139−141 dec	27	7.5	81
8	$CH_2N(Me)CH_2COOMe$	227−230 dec		3.4	9.6
9	$CH_2N(Me)CH_2COOH$	240 dec	1.5	0.72	584

[a] IC_{50}, concentration of drug (nM) to inhibit the phosphorylation of a random polyglutamic acid/tyrosine copolymer by EGFR, prepared from human A431 carcinoma cell vesicles by immunoaffinity chromatography; see the Experimental Section for details. Values are the averages from at least two independent dose−response curves; variation was generally ±15%. [b] HCl salt. [c] DiHCl salt.

each compound, and the resulting IC_{50}s listed in Table 1 are the average of at least two such determinations. As noted above, both previous SAR for the general class of 4-(phenylamino)quinazolines and molecular modeling studies suggested significant bulk tolerance at the 6/7-positions, allowing compounds such as the 6,7-diethoxyquinazoline **13** and the tricyclic derivatives **2a** and **3a** to retain high potency. In the present study, the N-substituted pyrazolo and pyrrolo compounds listed in Table 2 were prepared to probe the extent of this bulk tolerance and to provide more water-soluble analogues. The solubilities of selected compounds were determined by HPLC following sonication for 30 min at 20 °C. Lactate buffer (0.05 M) was used for compounds with neutral side chains and water for hydrochloride salts of amines and sodium salts of acids.

In the N-substituted pyrazolo series, the NMe analogue **2b** had similar potency to **2a**, showing that an H-bond donation here is not critical. The diol **2c** was prepared to retain a noncharged side chain but did not show improved solubility. As expected, the strongly basic $(CH_2)_2NMe_2$ side chain in **2d** did provide much more solubility (36 mM), but the compound was about 100-fold less potent than **2a**. The weakly basic morpholide side chain analogue **2f** was much more active, with an IC_{50} of 3.7 nM. Finally, the anionic CH_2COOH compound **2h** was much less effective.

In the pyrrolo series (**3a**−**h**), the parent compound **3a** was appreciably more soluble than the corresponding pyrazolo analogue **2a**. Substitution of the pyrrole nitrogen with Me in **3b** again resulted in little loss of activity. However, in this case the larger propanediol substituent had lesser effect on potency, with **3c** also being only 4-fold less potent than **3a**, with an IC_{50} of 1.6 nM. Again, the strongly basic $(CH_2)_2NMe_2$ side chain resulted in a considerable loss of potency for **3d**, while the longer chain homologue **3e** was slightly more effective. The more weakly basic ethylmorpholide **3f** was the best of the basic analogues, being only 8-fold less potent than **3a**, but both morpholide analogues (**3f**,**g**) were much less soluble than the more strongly basic compounds. The anionic derivative **3h** also retained moderate activity (IC_{50} 5.1 nM) and good solubility. Finally, the 3-substituted pyrrolo series (**4**−**9**) was overall the most effective, with IC_{50}s averaging about 4 nM. No clear trend was present, with the anionic derivative **9** in this case being the most effective, with an IC_{50} of 0.72 nM.

To see whether the EGFR binding model proposed above was consistent with these results, manual docking studies were performed to explore the fit of these compounds to the enzyme. Different initial orientations of the aromatic rings were used for selected bicyclic quinazolines and tricyclic pyrrolo- and pyrazoloquinazolines. Amino acid side chains were reoriented to relieve unfavorable steric interactions, and the complexes were subsequently energy minimized. Only SAR data were considered as criteria in choosing the most plausible complex because of the inability of current force fields to reproduce the large induced fit (and therefore correct enzyme−inhibitor interaction energies) of these enzymes upon ligand binding.

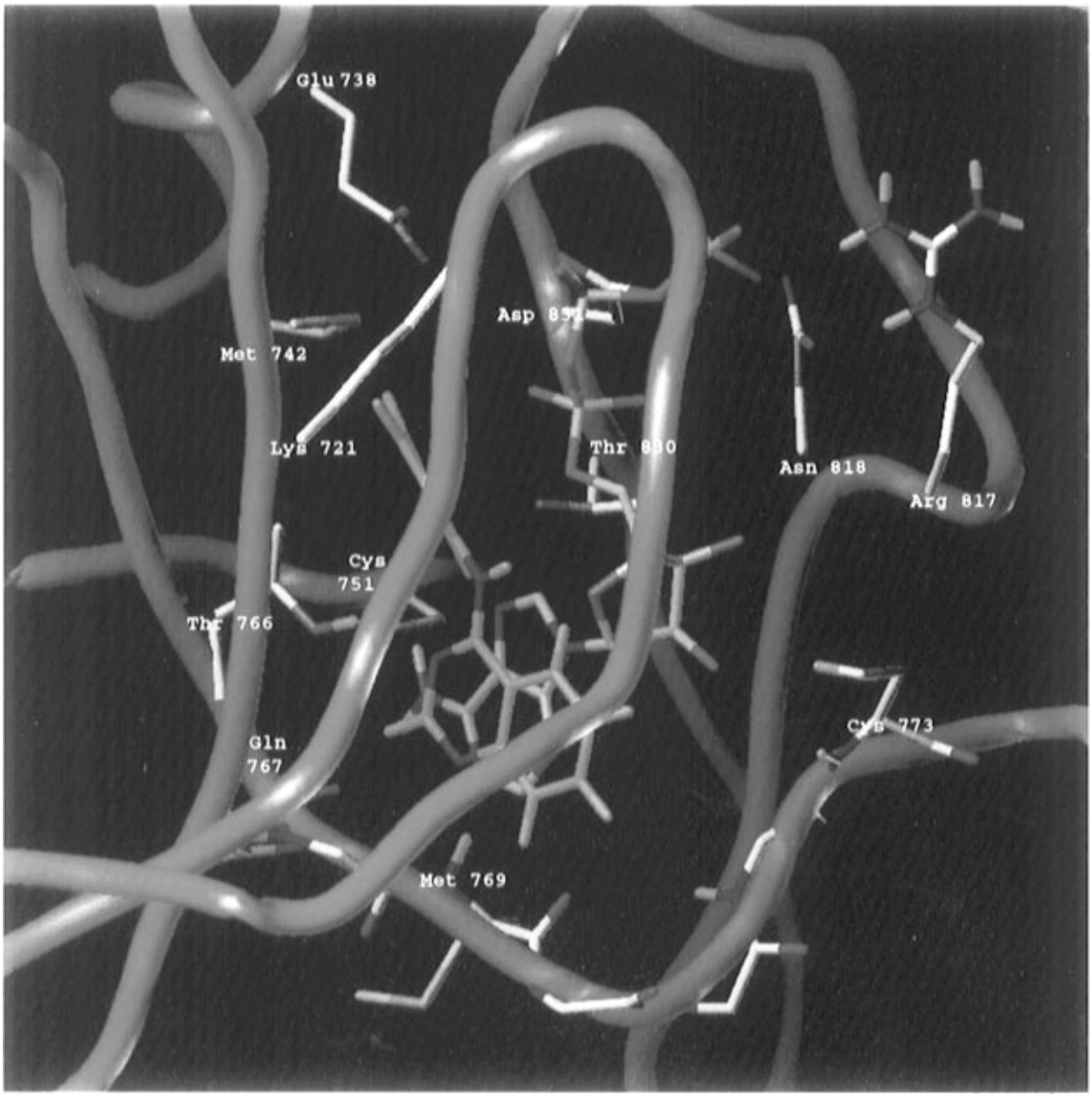

Figure 1. Superposition of compound **10** (green) and ATP (cyan) in the EGFR TK. In particular, the 4-[(3-bromophenyl)amino] substituent binds to a hydrophobic pocket deep in the binding cleft, which is not used by ATP.

Only one binding mode was found that satisfied all the SAR data described above and that had no major unfavorable steric interactions. In this binding mode (illustrated with **10** in Figure 1), the bicyclic (or tricyclic) chromophore binds to a narrow hydrophobic pocket in the N-terminal domain of EGFR TK, which is the binding site of the adenine base of ATP. The N-1 of the quinazoline ring forms a hydrogen bond with the NH backbone of Met-769. The NH backbone of this amino acid residue normally hydrogen bonds to N-1 of the adenine ring in ATP and helps to fix it in the binding pocket. This hydrogen bond is crucial for orienting the quinazoline ring in the pocket as demonstrated by more than a 3700-fold loss in inhibitory potency upon substitution of N-1 for a carbon atom. A second hydrogen bond can be formed with N-3 of the quinazoline ring and the side chain of Thr-766, which is located at the beginning of the extended coil stretch deep in the binding cleft. Removal of the N-3 of the quinazoline ring results in a moderate loss of affinity (a 200-fold loss in inhibitory potency) indicating that this hydrogen bond is probably less important. The 4-(3-bromoanilino) substituent is located in a deep, moderately sized pocket adjacent to the adenine binding pocket. The bottom of this inhibitor pocket is made up of Thr-766 (strand 5), Cys-751 (strand 4), Thr-830, and Met-742 (helix αC). The top of this pocket is more hydrophilic with Glu-738 (helix αC), Lys-721 (strand 3), and Asp-831 (strand 8).

The 4-(phenylamino)quinazolines, but not ATP, interact specifically with this pocket. The 4-(3-bromoanilino) substituent is adjacent to Cys-751 and Met-742 and can form favorable sulfur−aromatic interactions. The amino acid composition of the bottom of this pocket is unique to EGFR TK. In particular, a cysteine residue (Cys-751) is present only in the EGFR TK, which might explain part of the selectivity of this class of compounds for EGFR. The fact that there are very limited sites for favorable substitution off the 4-(3-bromoanilino) ring is in agreement with the restricted size of this pocket. The additional binding energy provided by the 4-(3-bromoanilino) substituent in this deep pocket may be the reason for the extremely high binding affinity of these small molecules. In comparison, the much less potent (micromolar range) competitive inhibitors iso-

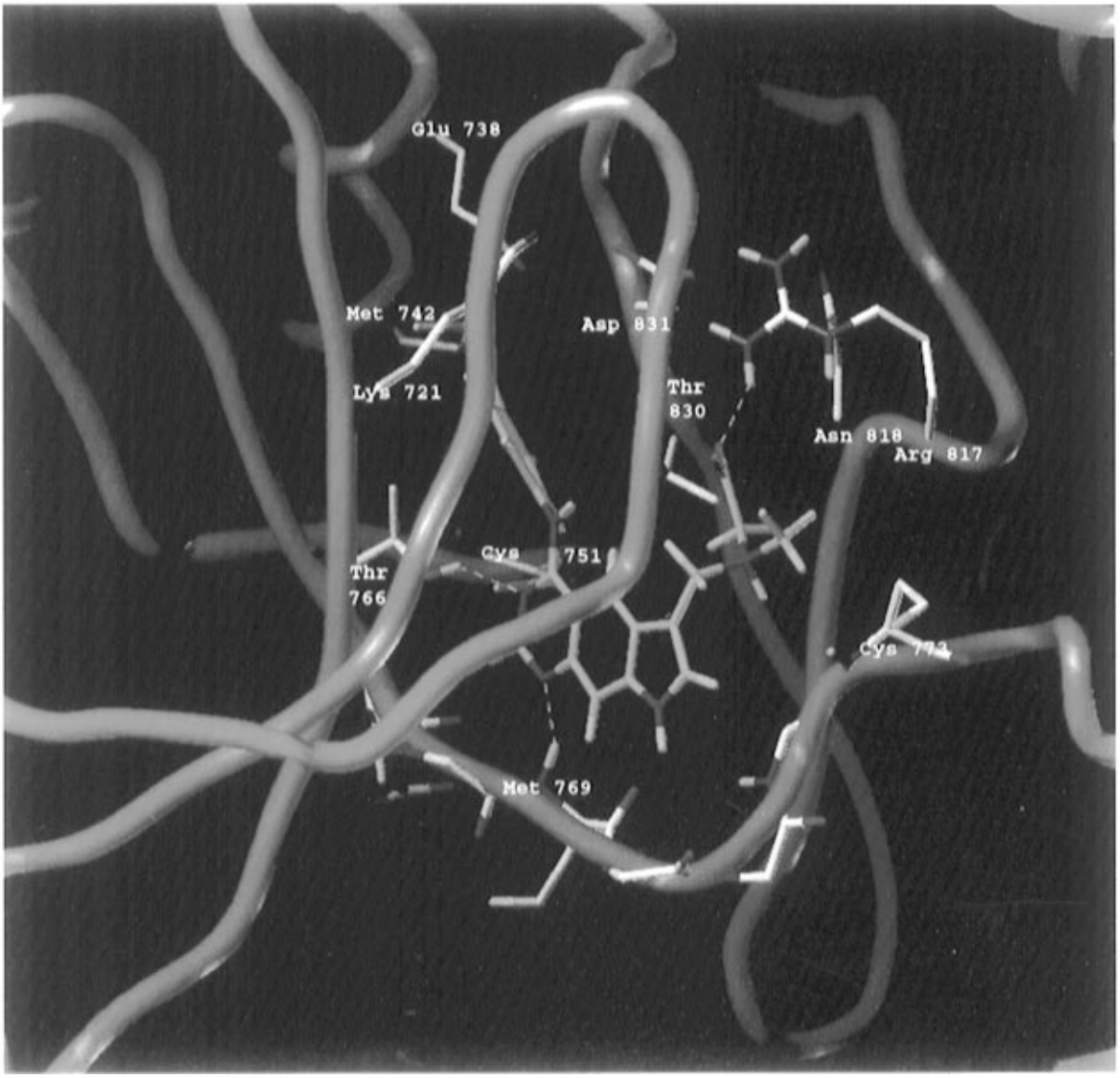

Figure 2. Compound **9** docked into the ATP binding site of the EGFR TK. The N-1 of the quinazoline ring forms a hydrogen bond with the NH backbone of Met-769. A second hydrogen bond can be formed with N-3 of the quinazoline ring and the side chain of Thr-766, located at the end of strand 5 deep in the binding cleft. The C-3 substituent of the pyrrole ring is located in a pocket corresponding to the ribose binding site of ATP and can form electrostatic interactions with Arg-817. In N-substituted pyrroloquinazolines, the substituents extend out of the binding pocket and do not participate in specific interactions with the enzyme.

pentyladenine (**17**) and olomucine (**18**) do not occupy the corresponding hydrophobic pocket when complexed with CDK2, binding closer to the entrance of the ATP binding site and making fewer hydrophobic contacts.

The model predicts that substitution of H-2 or H-8 in the quinazoline ring will be detrimental to binding, as shown by previous SAR data.[9] Both of the corresponding carbon atoms are located close to the peptide backbone of the extended coil stretch, and their substitution would prevent proper hydrogen bonding of N-1 and N-3 of the quinazoline ring with the extended coil stretch (Figure 1). Loss of potency upon substitution of C-8 with aza[11] is also explained by this binding mode, where the aza is located close to the carbonyl oxygen of Met-769 at the bottom of the cleft, leading to unfavorable repulsive electrostatic interactions (Figure 1). The model also predicts that large substituents at C-6 and C-7 of the quinazoline and pyrido[*d*]pyrimidines and at C-3 and (to some extent) N-1 of the tricyclic pyrrolo- and pyrazoloquinazolines can be tolerated without a major loss of affinity.

This is consistent with the present results (Table 2), which show that some N-1- and C-3-substituted pyrroloquinazolines in particular (e.g., **3c**,**f**, **5**, and **9**) retain high potency against the enzyme. This is consistent with an enzyme−inhibitor complex in which the 3-substituted pyrrole ring is occupying the entrance of the ATP binding pocket, with the pyrrolo NH located at the bottom of the cleft close to the extended coil stretch. The C-3 side chain in compound **9** is thus located in a pocket corresponding to the ribose binding site of ATP and can form electrostatic interactions with Arg-817 located on the catalytic loop. Additional interactions might occur with Cys-773 on the extended coil stretch (Figure 2). On the other hand, N-1-substituted pyrroloquinazolines are on average somewhat less active than the parent **3a**, with only the smallest substituent (methyl) being tolerated without loss of activity. The loss of potency

with longer, bulkier alkyl side chains might be due to unfavorable steric interactions with the bottom of the pocket. This causes a slight reorientation of the molecule in the binding site as is apparent from docking studies. In the enzyme−inhibitor complex, long alkyl side chains extend out of the binding pocket and do not participate in specific interactions with the enzyme.

The compounds were also evaluated for their ability to inhibit the autophosphorylation of EGFR in EGF-stimulated A431 cells in culture, quantitating the response by Western blotting. Both parent compounds **2a** and **3a** showed reasonable potency in this assay (ca. 20 nM), and the pyrrolo C-2 morpholide **3f**, which was also the most potent against the isolated enzyme, was slightly superior with an IC_{50} of 16 nM. Overall, for the N-substituted pyrazolo and pyrrolo compounds **2** and **3**, there was a good correlation between potency for inhibition of autophosphorylation in cells and inhibition of phosphorylation by the isolated enzyme (eq 1). The

$$\log(IC_{50}(\text{autophos})) = 0.67(\pm 0.12) \log(IC_{50}(\text{enzyme})) + 1.47(\pm 0.11)$$
$$n = 13,\ r = 0.87,\ F_{2,11} = 33,\ p = 0.001 \qquad (1)$$

only exception to this was the pyrrolo acid derivative **3h**, which was less active than predicted in the autophosphorylation assay and was not used in the derivation of eq 1. Previous studies[22] with acid derivatives have also shown that they have poorer cellular activity than predicted by their inhibition of the isolated enzyme, presumably due to low uptake into cells. This equation agrees well with one derived previously for related pyridopyrimidines:[11]

$$\log(IC_{50}(\text{autophos})) = 0.98 \log(IC_{50}(\text{enzyme})) + 0.81 \qquad (2)$$

However, the autophosphorylating activity of the 3-substituted pyrrolo compounds **4**−**9** was not well fitted by eq 1 and even within this series was not well correlated with enzyme IC_{50}. The strong base analogue **5**, the weak base **6**, and the neutral ester **8** all showed autophosphorylation activity superior to that of the parent compound **3a**, with IC_{50}s below 10 nM.

Conclusions

An efficient synthetic route has been developed for N-1-substituted pyrroloquinazolines, via alkylation of the thioether **21**. C-3 Mannich base analogues can also be readily prepared from the preformed compound **3a**. This allowed the preparation of a series of analogues bearing quite bulky solubilizing side chains at these positions. Some of these, particularly the C-3 analogues, retained high potency against the isolated enzyme. A molecular model of the EGFR TK was constructed from SAR data for inhibition of the EGFR by 4-(phenylamino)quinazolines and analogues and from structural information (particularly for the catalytic subunit of the cAMP-dependent protein kinase[17]). Using this model, a possible binding mode for this class of tricyclic inhibitors was identified, where the pyrrolo or pyrazolo ring occupies the entrance of the ATP binding pocket of the enzyme, with the nitrogen located at the bottom of the cleft and the C-3 position pointing toward a pocket corresponding to the ribose binding site of ATP. This allows considerable bulk tolerance for C-3 substituents and lesser but still significant bulk tolerance for N-1 substituents. The data for inhibition of substrate phosphorylation by EGFR are consistent with this binding model. A similar approach has recently been reported[23] to construct a binding model for the dianilinophthalimide EGFR inhibitor CGP 52411.

This binding model is different to one published recently by the Ciba-Geigy group for a series of related 4-(phenylamino)pyrrolopyrimidines.[24] In their model, the pyrrolopyrimidine chromophore is rotated through 180°, placing the 4-(phenylamino) substituent at the entrance of the ATP binding pocket, occupying the ribose binding site. The extensive SAR data presented in the current paper clearly exclude this binding mode. In particular, the N-substituted pyrroloquinazolines are unable to bind in their proposed binding mode, due to steric interference of the N-1 substituents with strands 4 and 5 and the extended coil stretch. The correlation between inhibition of isolated enzyme and inhibition of autophosphorylation for the N-substituted tricyclic compounds is similar to that seen previously for pyridopyrimidines. This suggests that the two classes of compounds function similarly and that similar solubilizing functions might be acceptable in both classes. However, the unexpectedly high potencies of the C-3-substituted compounds in the autophosphorylation assay show that activity against the isolated enzyme does not always predict well for activity in cells and, therefore, make these compounds of particular interest.

Experimental Section

Analyses were carried out in the Microchemical Laboratory, University of Otago, Dunedin, NZ. Melting points were determined on an Electrothermal 9200 melting point apparatus. NMR spectra were obtained on a Bruker AC-200 or AM-400 spectrometer and are referenced to Me_4Si for organic solutions and sodium 3-(trimethylsilyl)propanesulfonate for D_2O solutions. Thin-layer chromatography was carried out on aluminum-backed silica gel plates (Merck 60 F_{254}). Flash column chromatography was carried out on Merck silica gel (230−400 mesh). Petroleum ether refers to the fraction boiling at 40−60 °C. Mass spectra were recorded on a Varian VG 7070 spectrometer at nominal 5000 resolution.

5-[(3-Bromophenyl)amino]pyrrolo[3,2-*g*]quinazoline-1-acetic Acid (3h): Scheme 1. A solution of the known[10,15] pyrroloquinazoline **3a** (0.10 g, 0.29 mmol) in DMF (1 mL) was added dropwise under nitrogen to a suspension of NaH (14.1 mg of a 60% dispersion in oil, 0.35 mmol) in THF (1 mL). After 5 min, ethyl bromoacetate (36 μL, 0.32 mmol) was added, and the solution was stirred at 20 °C for 1.5 h. Water was added, and the mixture was extracted with EtOAc and worked up to give an oil which was chromatographed on silica gel. Elution with EtOAc/petroleum ether (1:4) gave a fraction enriched in the desired product, which was further purified by recrystallization from EtOAc/petroleum ether to give ethyl 5-[(3-bromophenyl)amino]pyrrolo[3,2-*g*]quinazoline-1-acetate (**3i**) (40 mg, 32%) as a cream solid: mp 194−196 °C; ^{1}H NMR ($CDCl_3$) δ 8.70 (br s, 1 H, NH), 8.12 (br s, 2 H), 7.71 (m, 2 H), 7.32 (d, J = 3.4 Hz, 1 H), 7.28−7.26 (m, 3 H), 6.69 (d, J = 3.4 Hz, 1 H), 4.90 (s, 2 H), 4.24 (q, J = 7.1 Hz, 2 H), 1.29 (t, J = 7.1 Hz, 3 H); ^{13}C NMR δ 168.11 (s), 152.69 (d), 145.15 (s), 140.63 (s), 140.10 (s), 133.52 (s), 130.25 (d), 130.07 (s), 126.88 (d), 124.27 (d), 122.62 (s), 119.87 (d), 111.82 (d), 109.97 (s), 105.67 (d), 102.90 (d), 62.05 (t), 47.85 (t), 14.13 (q). Anal. ($C_{20}H_{17}BrN_4O_2$) C, H, N.

A solution of **3i** (40 mg, 0.09 mmol) in MeOH (5 mL) was treated with 2 N NaOH (1 mL), and the mixture was stirred at 20 °C for 30 min. The MeOH was removed under reduced

pressure, and the remaining solution was carefully neutralized with 1 N HCl. The precipitated product was collected and washed well with water to give 5-[(3-bromophenyl)amino]-pyrrolo[3,2-*g*]quinazoline-1-acetic acid (**3h**) (28 mg, 78%): mp (MeOH) 175 °C dec; ^{1}H NMR [$(CD_3)_2SO$] δ 13.80 (br, 1 H), 10.63 (br, 1 H), 9.02 (s, 1 H), 8.73 (s, 1 H), 8.25 (s, 1 H), 7.92 (dt, J = 6.9, 1.8 Hz, 1 H), 7.84 (s, 1 H), 7.78 (d, J = 3.4 Hz, 1 H), 7.43−7.38 (m, 2 H), 6.84 (d, J = 3.4 Hz, 1 H), 5.22 (s, 2 H); ^{13}C NMR δ 169.97 (s), 158.88 (s), 150.73 (d), 140.41 (s), 140.28 (s), 135.59 (d), 130.40 (d), 129.48 (s), 126.89 (d), 125.19 (d), 121.66 (d), 121.11 (s), 115.11 (d), 108.37 (s), 102.10 (d), 102.00 (d), 47.35 (t). Anal. ($C_{18}H_{13}BrN_4O_2$) C, H, N.

Similar alkylation of the known[10] 5-[(3-bromophenyl)amino]-1*H*-pyrazolo[4,3-*g*]quinazoline (**2a**) with NaH and ethyl bromoacetate gave ethyl 5-[(3-bromophenyl)amino]-1*H*-pyrazolo-[4,3-*g*]quinazoline-1-acetate (**2i**) (58%): mp (EtOAc/petroleum ether) 191 °C; ^{1}H NMR ($CDCl_3$) δ 8.71 (s, 1 H), 8.29 (s, 2 H), 8.22 (s, 1 H), 8.08 (br s, 1 H), 7.77 (br s, 1 H), 7.72 (br d, J = 7.2 Hz, 1 H), 7.31−7.29 (m, 2 H), 5.24 (s, 2 H), 4.26 (q, J = 7.1 Hz, 2 H), 1.29 (t, J = 7.1 Hz, 3 H); ^{13}C NMR δ 167.82 (s), 158.34 (s), 154.72 (d), 142.01 (s), 139.51 (s), 135.47 (d), 130.31 (d), 127.53 (d), 124.80 (d), 124.60 (s), 122.63 (s), 120.41 (d), 114.05 (d), 111.01 (s), 105.08 (d), 62.16 (t), 50.37 (t), 14.12 (q). Anal. ($C_{19}H_{16}BrN_5O_2\cdot 0.5H_2O$) C, H.

Hydrolysis of **2i** as above gave 5-[(3-bromophenyl)amino]-pyrazolo[4,3-*g*]quinazoline-1-acetic acid (**2h**) (91%): mp (EtOAc) 252 °C dec; ^{1}H NMR [$(CD_3)_2SO$] δ 13.10 (br, 1 H), 10.12 (br, 1 H), 9.17 (s, 1 H), 8.61 (s, 1 H), 8.56 (s, 1 H), 8.32 (br s, 1 H), 8.04 (s, 1 H), 7.97 (d, J = 8.1 Hz, 1 H), 7.40−7.25 (m, 2 H), 5.42 (s, 2 H); ^{13}C NMR δ 158.71 (s), 153.91 (d), 146.66 (s), 141.82 (s), 141.05 (s), 136.62 (s), 135.24 (d), 130.35 (d), 125.95 (d), 124.17 (d), 123.85 (s), 121.13 (s), 120.70 (d), 116.71 (d), 110.70 (s), 104.82 (d), 49.98 (t); FABMS found $[M + H]^+$ 400.0230, 398.0203, $C_{17}H_{12}BrN_5O_2$ requires 400.0203, 398.0253. Anal. ($C_{17}H_{12}BrN_5O_2\cdot 0.5H_2O$) C, H.

5-[(3-Bromophenyl)amino]-1-methylpyrrolo[3,2-*g*]-quinazoline (3b): Scheme 2. A suspension of the known[15] pyrrolo[3,2-*g*]quinazolone **19** (1.55 g, 8.37 mmol) and P_2S_5 (3.72 g, 16.74 mmol) in pyridine (80 mL) was heated under reflux for 18 h and then concentrated to dryness. The residue was slurried in boiling water and filtered. The solid was dissolved in 1 N NaOH and filtered and the filtrate carefully neutralized with saturated aqueous NH_4Cl. The precipitated solid was collected and dried under vacuum to give 1*H*-pyrrolo[3,2-*g*]-quinazoline-5(6*H*)-thione (**20**) (1.54 g, 91%): mp >370 °C; ^{1}H NMR [$(CD_3)_2SO$] δ 13.50 (br, 1 H, exch with D_2O), 11.80 (br s, 1 H, exch with D_2O), 8.96 (s, 1 H), 8.08 (s, 1 H), 7.74 (s, 1 H), 7.73 (dd, J = 3.1, 2.4 Hz, 1 H), 7.40 (t, J = 50.8 Hz, 1 H), 6.80 (br s, 1 H); ^{13}C NMR δ 185.81 (s), 140.95 (s), 140.36 (d), 138.93 (s), 130.74 (d), 129.73 (s), 121.98 (s), 121.41 (d), 107.33 (d), 102.46 (d); DEIMS found M^+ 201.0367, $C_{10}H_7N_3S$ requires 201.0361.

Methyl iodide (0.42 mL, 6.78 mmol) was added to a solution of **20** (1.30 g, 6.46 mmol) and 1 N NaOH (9.00 mL, 9.00 mmol) in MeOH/water (1:1, 80 mL). The mixture was stirred at room temperature for 2 h, and the precipitate was filtered off and washed well with water to give 5-(methylthio)-1*H*-pyrrolo[3,2-*g*]quinazoline (**21**) (0.84 g, 60%): mp (MeOH) 278 °C dec; ^{1}H NMR [$(CD_3)_2SO$] δ 11.63 (br s, 1 H, exch with D_2O), 8.84 (s, 1 H), 8.37 (s, 1 H), 7.91 (s, 1 H), 7.80 (dd, J = 3.0, 2.4 Hz, 1 H), 6.80 (dd, J = 3.0, 0.9 Hz, 1 H), 2.71 (s, 3 H); ^{13}C NMR δ 170.08 (s), 150.36 (s), 142.09 (s), 140.59 (s), 131.96 (d), 129.90 (s), 117.26 (s), 113.73 (d), 106.85 (d), 101.79 (d), 11.97 (t). Anal. ($C_{11}H_9N_3S$) C, H, N, S.

A solution of **21** (0.10 g, 0.46 mmol) in DMF (1 mL) was added under nitrogen to a suspension of NaH (22 mg of a 60% dispersion in oil, 0.57 mmol) in THF (2 mL). After 5 min, methyl iodide (32 μL, 0.51 mmol) was added, and the solution was stirred at 20 °C for 30 min and then partitioned between EtOAc and water. Workup of the organic layer gave 1-methyl-5-(methylthio)pyrrolo[3,2-*g*]quinazoline (**22**) (0.10 g, 94%): mp (EtOAc/petroleum ether) 198−200 °C; ^{1}H NMR [$(CD_3)_2SO$] δ 8.86 (s, 1 H), 8.37 (s, 1 H), 7.97 (s, 1 H), 7.76 (d, J = 3.3 Hz, 1 H), 6.80 (d, J = 3.3 Hz, 1 H), 3.92 (s, 3 H), 2.71 (s, 3 H); ^{13}C NMR δ 170.29 (s), 150.60 (d), 142.11 (s), 140.90 (s), 136.06 (d), 130.05 (s), 117.20 (s), 114.22 (d), 105.48 (d), 101.24 (d), 32.79 (q), 12.03 (q). Anal. ($C_{12}H_{11}N_3S$) C, H, N.

A solution of thioether **22** (0.10 g, 0.44 mmol), 3-bromoaniline (0.10 mL, 0.96 mmol), and concentrated HCl (39 μL, 0.48 mmol) in *N*-methylpyrrolidinone (20 mL) was warmed at 120 °C for 4 h, then cooled, and poured into Et_2O (200 mL). After chilling at −20 °C overnight, the precipitated solid was filtered off and dissolved in hot MeOH, and the solution was basified with concentrated aqueous NH_3 and then concentrated to dryness. The residue was partitioned between EtOAc and water, and the organic portion was worked up and chromatographed on alumina. EtOAc/petroleum ether (1:1) gave foreruns, while EtOAc eluted 5-[(3-bromophenyl)amino]-1-methylpyrrolo[3,2-*g*]quinazoline (**3b**) (97 mg, 62%): mp (EtOAc/petroleum ether) 178−180 °C; ^{1}H NMR [$(CD_3)_2SO$] δ 9.81 (s, 1 H), 8.83 (s, 1 H), 8.56 (s, 1 H), 8.34 (t, J = 1.9 Hz, 1 H), 7.98 (dd, J = 7.2, 1.5 Hz, 1 H), 7.85 (s, 1 H), 7.70 (d, J = 3.2 Hz, 1 H), 7.36 (dd, J = 7.9, 7.2 Hz, 1 H), 7.28 (dd, J = 7.9, 1.5 Hz, 1 H), 6.75 (d, J = 3.2 Hz, 1 H), 3.91 (s, 3 H); ^{13}C NMR δ 157.82 (s), 151.75 (d), 144.60 (s), 141.56 (s), 140.29 (s), 134.93 (d), 130.30 (d), 128.93 (s), 125.35 (d), 123.71 (d), 121.14 (s), 120.26 (d), 113.69 (d), 109.32 (s), 105.18 (d), 100.88 (d), 32.72 (q). Anal. ($C_{17}H_{13}BrN_4\cdot H_2O$) C, H, N.

5-[(3-Bromophenyl)amino]-1-methylpyrazolo[4,3-*g*]-quinazoline (2b). Similar reaction of the known[10] 1*H*-pyrazolo[4,3-*g*]quinazolinone **23** with P_2S_5 gave 1*H*-pyrazolo-[4,3-g]quinazoline-5(6*H*)-thione (**24**) (85%): mp >400 °C; ^{1}H NMR [$(CD_3)_2SO$] δ 13.52 (br, 2 H), 9.18 (d, J = 0.7 Hz, 1 H), 8.52 (d, J = 0.7 Hz, 1 H), 8.15 (s, 1 H), 7.79 (s, 1 H); ^{13}C NMR δ 187.20 (s), 142.49 (s), 142.23 (d), 141.14 (s), 136.14 (d), 124.30 (s), 124.10 (d), 122.99 (s), 105.45 (d); DEIMS found M^+ 202.0310, $C_9H_6N_4S$ requires 202.0313.

Similar methylation of **24** gave 5-(methylthio)-1*H*-pyrazolo-[4,3-*g*]quinazoline (**25**) (58%): mp 380 °C dec; ^{1}H NMR [$(CD_3)_2$-SO] δ 13.53 (s, 1 H), 8.91 (s, 1 H), 8.75 (s, 1 H), 8.55 (s, 1 H), 7.99 (s, 1 H), 2.73 (s, 3 H); ^{13}C NMR δ 172.72 (s), 152.05 (d), 143.97 (s), 141.81 (s), 135.64 (d), 124.14 (s), 117.81 (d), 117.05 (s), 105.31 (d), 12.13 (q). Anal. ($C_{10}H_8N_4S$) C, H, N, S.

Similar reaction of **25** with NaH and MeI afforded 1-methyl-5-(methylthio)pyrazolo[4,3-*g*]quinazoline (**26**) (96%): mp (EtOAc) 202−203 °C; ^{1}H NMR ($CDCl_3$) δ 8.93 (s, 1 H), 8.62 (d, J = 0.9 Hz, 1 H), 8.30 (d, J = 0.9 Hz, 1 H), 7.89 (s, 1 H), 4.19 (s, 3 H), 2.76 (s, 3 H); ^{13}C NMR δ 173.81 (s), 152.83 (d), 144.72 (s), 141.89 (s), 134.41 (d), 124.86 (s), 118.90 (s), 117.53 (d), 104.80 (d), 35.81 (q), 12.69 (q). Anal. ($C_{11}H_{10}N_4S$) C, H, N.

Coupling of **26** with 3-bromoaniline as above gave 5-[(3-bromophenyl)amino]-1-methylpyrazolo[4,3-*g*]quinazoline (**2b**) (66%): mp (EtOAc/petroleum ether) 227−229 °C; ^{1}H NMR [$(CD_3)_2SO$] δ 10.05 (s, 1 H), 9.14 (s, 1 H), 8.61 (s, 1 H), 8.51 (d, J = 0.9 Hz, 1 H), 8.31 (t, J = 1.9 Hz, 1 H), 8.00 (d, J = 0.9 Hz, 1 H), 7.97 (br d, J = 8.0 Hz, 1 H), 7.38 (dd, J = 8.0, 7.9 Hz, 1 H), 7.31 (br d, J = 7.9 Hz, 1 H), 4.16 (s, 3 H); ^{13}C NMR δ 158.69 (s), 153.82 (d), 146.51 (s), 141.23 (s), 141.01 (s), 134.14 (d), 130.31 (d), 125.89 (d), 124.13 (d), 123.63 (s), 121.11 (s), 120.65 (d), 116.58 (d), 110.48 (s), 104.46 (d), 35.48 (q). Anal. ($C_{16}H_{12}$-BrN_5) C, H, N.

5-[(3-Bromophenyl)amino]-1-(2,3-dihydroxypropyl)-pyrrolo[3,2-*g*]quinazoline (3c). A solution of the pyrroloquinazoline **21** (0.20 g, 0.93 mmol) in DMF (2 mL) was added dropwise under nitrogen to a suspension of NaH (0.11 g of a 60% dispersion in mineral oil, 2.79 mmol) in THF (2 mL). After 10 min, 1-chloropropane-2,3-diol (85 μL, 1.02 mmol) was added, and the solution was warmed at 45 °C for 30 min. Water was added, and the mixture was extracted into EtOAc, worked up, and chromatographed on silica gel. EtOAc eluted starting material (90 mg, 45%), while MeOH/EtOAc (1:9) gave 1-(2,3-dihydroxypropyl)-5-(methylthio)pyrrolo[3,2-*g*]quinazoline **(27)** (70 mg, 26%): mp (trituration with Me_2CO) 198−200 °C; ^{1}H NMR [$(CD_3)_2SO$] δ 8.85 (s, 1 H), 8.36 (s, 1 H), 8.03 (s, 1 H), 7.75 (d, J = 3.2 Hz, 1 H), 6.80 (d, J = 3.2 Hz, 1 H), 5.06 (d, J = 5.2 Hz, 1 H, OH), 4.86 (t, J = 5.6 Hz, 1 H, OH), 4.44 (dd, J = 14.4, 3.6 Hz, 1 H), 4.20 (dd, J = 14.4, 7.3 Hz, 1 H), 3.86 (m, 1 H), 3.41 (m, 2 H), 2.71 (s, 3 H); ^{13}C NMR δ 170.09 (s), 150.50 (d), 142.01 (s), 140.81 (s), 136.12 (d), 130.09 (s), 117.13 (s), 113.98 (d), 105.94 (d), 101.12 (d), 70.60 (d), 63.22 (t), 49.19 (t), 11.98 (q). Anal. ($C_{14}H_{15}N_3O_2S\cdot 0.5H_2O$) C, H, N, S.

A solution of diol **27** (0.15 g, 0.52 mmol), 3-bromoaniline (0.12 mL, 1.14 mmol), and concentrated HCl (51 μL, 0.57 mmol) in *N*-methylpyrrolidinone (8 mL) was warmed at 120 °C for 15 h, then cooled, and poured into Et_2O (300 mL). The resulting precipitate was filtered off, dissolved in hot propan-2-ol/water (1:1), and basified with concentrated NH_3. The resulting solution was concentrated to dryness, and the residue was triturated with water, dissolved in EtOAc/MeOH (9:1), and chromatographed on silica gel. Elution with EtOAc gave foreruns, while EtOAc/MeOH (19:1) eluted 5-[(3-bromophenyl)-amino]-1-(2,3-dihydroxypropyl)pyrrolo[3,2-*g*]quinazoline (**3c**) as a yellow solid (84 mg, 39%). This was converted immediately into the hydrochloride salt by dissolution in MeOH (1 mL), addition of concentrated HCl (1 drop), and cooling at −20 °C for 48 h. The salt was filtered off and washed well with Et_2O: mp 184−187 °C; ^{1}H NMR [$(CD_3)_2SO$] δ 14.89 (br, 1 H), 11.44 (s, 1 H), 9.15 (s, 1 H), 8.94 (s, 1 H), 8.12 (t, J = 1.9 Hz, 1 H), 7.97 (s, 1 H), 7.87 (d, J = 3.4 Hz, 1 H), 7.81 (br d, J = 8.2 Hz, 1 H), 7.53 (br d, J = 8.1 Hz, 1 H), 7.48 (dd, J = 8.2, 8.1 Hz, 1 H), 6.92 (d, J = 3.4 Hz, 1 H), 5.10 (br, 2 H, OH), 4.46 (dd, J =14.5, 2.6 Hz, 1 H), 4.25 (dd, J = 14.5, 7.2 Hz, 1 H), 3.87 (m, 1 H), 3.40 (dd, J =11.0, 5.2 Hz, 1 H), 3.31 (dd, J =11.0, 6.5 Hz, 1 H); ^{13}C NMR δ 160.26 (s), 149.41 (d), 140.59 (s), 138.71 (s), 136.60 (d), 130.62 (d), 130.04 (s), 128.80 (d), 126.99 (d), 123.36 (d), 121.13 (s), 116.42 (d), 106.60 (s), 102.11 (d), 98.35 (d), 70.65 (d), 63.01 (t), 49.37 (t). Anal. ($C_{19}H_{17}BrN4O_2$·HCl) C, H, N, S.

Similar alkylation of the pyrazoloquinazoline **25** with 1-chloropropane-2,3-diol followed by reaction of the resultant crude thioether **28** with 3-bromoaniline afforded 5-[(3-bromophenyl)amino]-1-(2,3-dihydroxypropyl)pyrazolo[4,3-*g*]quinazoline (**2c**): mp (EtOAc) 175−180 °C dec; ^{1}H NMR [$(CD_3)_2SO$] δ 11.36 (s, 1 H), 9.12 (s, 1 H), 8.61 (s, 1 H), 8.53 (d, J = 0.9 Hz, 1 H), 8.32 (t, J = 1.8 Hz, 1 H), 8.00 (d, J = 0.9 Hz, 1 H), 7.95 (d, J = 8.0 Hz, 1 H), 7.40 (dd, J = 8.0, 7.9 Hz, 1 H), 7.30 (d, J = 7.9 Hz, 1 H), 5.05 (d, J = 5.1 Hz, 1 H, OH), 4.89 (t, J = 5.6 Hz, OH), 4.45 (dd, J = 14.6, 2.5 Hz, 1 H), 4.25 (dd, J = 14.6, 7.1 Hz, 1 H), 3.87 (m, 1 H), 3.35 (m, 2 H). Anal. ($C_{18}H_{16}BrN_5O_2$·0.5H_2O) C, H.

5-[(3-Bromophenyl)amino]-1-[2-(*N*,*N*-dimethylamino)-ethyl]pyrrolo[3,2-*g*]quinazoline (3d): General Example of Scheme 3. A mixture of the pyrroloquinazoline **3a** (0.10 g, 0.29 mmol), 2-(dimethylamino)ethyl chloride hydrochloride (51 mg, 0.35 mmol), $CsCO_3$ (0.13 g, 0.41 mmol), and powdered 4A molecular sieves (0.20 g) in dry Me_2CO (10 mL) was heated under reflux for 6 h. Additional equivalents of alkylating agent and $CsCO_3$ were added, and the mixture was heated under reflux overnight. After concentration under reduced presssure, the residue was partitioned between EtOAc and water and then filtered. The organic layer was worked up and chromatographed on silica gel. EtOAc eluted unreacted **3a** (11 mg, 11%), while EtOAc/MeOH/concentrated NH_3 (9:1:trace) eluted material which was rechromatographed on alumina. Elution with EtOAc/petroleum ether (2:3) gave pure 5-[(3-bromophenyl)amino]-1-[2-(*N*,*N*-dimethylamino)ethyl]pyrrolo-[3,2-*g*]quinazoline (**3d**) (23 mg, 19%): mp (EtOAc/petroleum ether) 150−152 °C; ^{1}H NMR ($CDCl_3$) δ 8.72 (s, 1 H), 7.72 (br s, 2 H), 7.43 (d, J = 3.2 Hz, 1 H), 7.28 (m, 2 H), 6.68 (d, J = 3.2 Hz, 1 H), 4.31 (t, J = 6.9 Hz, 2 H), 2.76 (t, J = 6.9 Hz, 2 H), 2.31 (s, 6 H); ^{13}C NMR δ 152.58 (s), 146.32 (d), 140.20 (s), 133.83 (s), 133.45 (d), 130.25 (d), 129.84 (s), 126.81 (d), 124.22 (d), 122.64 (s), 119.81 (d), 111.50 (d), 105.85 (d), 101.72 (d), 58.43 (t), 45.62 (q), 44.88 (t). Anal. ($C_{18}H_{16}BrN_5O_2$·0.5H_2O) C, H; N: found, 15.9; calcd, 16.5.

The following 1-substituted pyrrolo- and pyrazoloquinazolines were synthesized in a similar manner. Purification was best achieved by sequential chromatography on silica gel and alumina as described above followed by recrystallization from EtOAc/petroleum ether.

5-[(3-Bromophenyl)amino]-1-[3-(*N*,*N*-dimethylamino)-propyl]pyrrolo[3,2-*g*]quinazoline (3e) (26%): mp 171−172 °C; ^{1}H NMR [$(CD_3)_2SO$] δ 9.81 (s, 1 H), 8.83 (s, 1 H), 8.56 (s, 1 H), 8.36 (t, J = 1.8 Hz, 1 H), 8.00 (br d, J = 8.0 Hz, 1 H), 7.89 (s, 1 H), 7.74 (d, J = 3.3 Hz, 1 H), 7.36 (dd, J = 8.0, 8.0 Hz, 1 H), 7.27 (br d, J = 8.0 Hz, 1 H), 6.76 (d, J = 3.3 Hz, 1 H), 4.33 (t, J = 6.8 Hz, 2 H), 2.17 (t, J = 6.9 Hz, 2 H), 2.12 (s, 6 H), 1.93 (m, 2 H); ^{13}C NMR δ 157.74 (s), 151.72 (d), 144.59 (s), 141.57 (s), 139.67 (s), 134.02 (d), 130.25 (d), 128.96 (s), 125.28 (d), 123.64 (d), 121.12 (s), 120.18 (d), 113.73 (d), 109.32 (s), 105.22 (d), 101.11 (d), 55.80 (t), 45.06 (q), 43.55 (t), 27.47 (t). Anal. ($C_{21}H_{22}BrN_5$) C, H, N.

5-[(3-Bromophenyl)amino]-1-[2-(4-morpholino)ethyl]-pyrrolo[3,2-*g*]quinazoline (3f) (19%): mp 114−116 °C; ^{1}H NMR ($CDCl_3$) δ 8.74 (s, 1 H), 8.17 (s, 1 H), 8.14 (br s, 1 H), 7.87 (s, 1 H), 7.73 (m, 1 H), 7.58 (br, 1 H), 7.45 (d, J = 3.4 Hz, 1 H), 7.28 (m, 2 H), 6.70 (d, J = 3.4 Hz, 1 H), 4.34 (t, J = 6.7 Hz, 2 H), 2.50 (t, J = 4.6 Hz, 4 H); ^{13}C NMR δ 157.49 (s), 152.66 (d), 145.02 (s), 140.86 (s), 140.13 (s), 133.50 (d), 130.26 (d), 129.82 (s), 126.85 (d), 124.20 (d), 122.65 (s), 119.77 (d), 111.38 (d), 109.66 (s), 105.97 (d), 101.67 (d), 66.95 (t), 57.67 (t), 53.82 (t), 44.31 (t). Anal. ($C_{22}H_{22}BrN_5$·0.5H_2O) C, H, N.

5-[(3-Bromophenyl)amino]-1-[3-(4-morpholino)propyl]-pyrrolo[3,2-*g*]quinazoline (3g) (34%): mp 147−149 °C; ^{1}H NMR ($CDCl_3$) δ 8.73 (s, 1 H), 8.17 (s, 1 H), 8.13 (br s, 1 H), 7.89 (s, 1 H), 7.72 (m, 1 H), 7.62 (br, 1 H), 7.39 (d, J = 3.3 Hz, 1 H), 7.28 (m, 2 H), 6.67 (d, J = 3.3 Hz, 1 H), 4.31 (t, J = 6.7 Hz, 2 H), 3.72 (t, J = 4.6 Hz, 4 H), 2.38 (t, J = 4.6 Hz, 4 H), 2.27 (t, J = 6.9 Hz, 2 H), 2.05 (dt, J = 6.9, 6.7 Hz, 2 H); ^{13}C NMR δ 157.51 (s), 152.58 (d), 144.92 (s), 140.24 (s), 140.16 (s), 133.37 (d), 103.25 (d), 129.82 (s), 126.81 (d), 124.21 (d), 122.64 (s), 119.79 (d), 111.36 (d), 109.58 (s), 106.17 (d), 101.54 (d), 66.97 (t), 55.16 (t), 53.55 (t), 44.23 (t), 26.43 (t). Anal. ($C_{23}H_{24}$-BrN_5O·0.5H_2O) C, H, N.

5-[(3-Bromophenyl)amino]-1-[2-(*N*,*N*-dimethylamino)-ethyl]pyrazolo[4,3-*g*]quinazoline (2d) (12%): converted into the hydrochloride salt and crystallized from MeOH/Et_2O; mp 262−264 °C; ^{1}H NMR [$(CD_3)_2SO$] δ 10.89 (br, 1 H), 9.95 (s, 1 H), 9.07 (s, 1 H), 8.65 (s, 1 H), 8.64 (s, 1 H), 8.37 (s, 1 H), 8.01 (d, J = 8.4 Hz, 1 H), 7.36 (dd, J = 8.4, 7.9 Hz, 1 H), 7.29 (br d, J = 7.9 Hz, 1 H), 4.77 (t, J = 6.7 Hz, 2 H), 3.46 (br, 2 H), 2.73 (s, 6 H); ^{13}C NMR δ 158.08 (s), 152.46 (d), 149.20 (d), 145.39 (s), 142.97 (s), 141.26 (s), 138.14 (s), 130.29 (d), 125.63 (d), 123.86 (d), 121.12 (s), 120.41 (d), 112.78 (d), 111.12 (s), 106.68 (d), 54.98 (t), 42.91 (q), 39.96 (t). Anal. ($C_{19}H_{19}BrN_6$·-HCl·H_2O) C, H, N, Cl.

5-[(3-Bromophenyl)amino]-1-[2-(4-morpholino)ethyl]-pyrazolo[4,3-*g*]quinazoline (2f) (21%): converted into the hydrochloride salt; mp (EtOAc/petroleum ether) 216−220 °C; ^{1}H NMR [$(CD_3)_2SO$] δ 10.07 (br s, 1 H), 9.15 (s, 1 H), 8.61 (s, 1 H), 8.53 (s, 1 H), 8.31 (br s, 1 H), 8.07 (s, 1 H), 7.96 (d, J = 7.3 Hz, 1 H), 7.33 (m, 2 H), 4.68 (t, J = 6.4 Hz, 2 H), 3.50 (t, J = 4.2 Hz, 4 H), 2.87 (t, J = 6.4 Hz, 2 H), 2.50 (t, J = 4.2 Hz, 4 H); ^{13}C NMR δ 153.81 (d), 141.23 (s), 134.59 (d), 130.61 (d), 130.35 (d), 125.96 (d), 124.20 (d), 123.69 (s), 121.13 (s), 120.72 (d), 117.70 (s), 116.66 (s), 115.78 (s), 112.63 (d), 104.65 (d), 65.95 (t), 57.02 (t), 53.08 (t), 45.71 (t); DEIMS found M^+ 454.0965, 452.0969, $C_{21}H_{21}BrN_6O$ requires 454.0940, 452.0960. Anal. ($C_{21}H_{21}BrN_6O$·2HCl·H_2O) C, H.

5-[(3-Bromophenyl)amino]-3-[(N^1,N^1,*N*-trimethylethyl-enediamino)methyl]pyrrolo[3,2-*g*]quinazoline (7): General Example of Scheme 4. A solution of pyrroloquinazoline **3a** (0.14 g, 0.41 mmol), formaldehyde (24 μL of a 40% aqueous solution, 0.45 mmol), and *N*,*N*,*N*′-trimethylethylenediamine (57 μL, 0.45 mmol) was warmed at 50 °C for 1 h. A further equivalent each of formaldehyde and amine was added, and warming was continued for a further 2 h. One drop of concentrated NH_4OH was added, and the solution was concentrated to dryness onto alumina and chromatographed directly. EtOAc eluted a trace of starting material, while MeOH/EtOAc (1:19) eluted 5-[(3-bromophenyl)amino]-3-[(N^1,N^1,*N*-trimethylethylenediamino)methyl]pyrrolo[3,2-*g*]-quinazoline (**7**) as a yellow oil (77 mg, 41%). Dissolution in EtOAc followed by precipitation with petroleum ether afforded crystalline methanol solvate: mp 139−141 °C dec; ^{1}H NMR [$(CD_3)_2SO$] δ 11.33 (s, 1 H), 9.81 (s, 1 H), 8.81 (s, 1 H), 8.51 (s, 1 H), 8.27 (t, J = 1.8 Hz, 1 H), 7.98 (d, J = 8.2 Hz, 1 H), 7.74 (s, 1 H), 7.58 (d, J = 2.0 Hz, 1 H), 7.37 (dd, J = 8.2, 8.1 Hz, 1 H), 7.28 (br d, J = 8.1 Hz, 1 H), 3.82 (s, 2 H), 2.51 (t, J = 7.6 Hz, 2 H), 2.40 (t, J = 7.6 Hz, 2 H), 2.25 (s, 3 H), 2.11 (s, 6 H); ^{13}C NMR δ 157.78 (s), 151.46 (d), 144.62 (s), 141.51 (s), 140.26 (s), 130.24 (d), 129.44 (d), 129.10 (s), 125.39 (d), 123.95 (d), 121.08 (s), 120.54 (d), 112.08 (d), 112.00 (s), 109.00 (s), 106.53

(d), 56.98 (t), 54.46 (t), 52.42 (t), 45.46 (q), 42.16 (q). Anal. ($C_{22}H_{25}BrN_6$·MeOH) C, H, N.

The following 3-substituted pyrrolo[3,2-*g*]quinazolines were prepared in a similar manner by reaction of the parent heterocycle with formaldehyde and the appropriate secondary amine.

5-[(3-Bromophenyl)amino]-3-[(*N*,*N*-dimethylamino)-methyl]pyrrolo[3,2-*g*]quinazoline (5) (34%): mp (EtOAc/petroleum ether) 220 °C dec; ^{1}H NMR [$(CD_3)_2SO$] δ 11.35 (s, 1 H), 9.86 (s, 1 H), 8.83 (s, 1 H), 8.53 (s, 1 H), 8.28 (t, J = 1.6 Hz, 1 H), 7.98 (br d, J = 8.5 Hz, 1 H), 7.76 (s, 1 H), 7.59 (d, J = 2.0 Hz, 1 H), 7.37 (dd, J = 8.5, 8.2 Hz, 1 H), 7.29 (br d, J = 8.2 Hz, 1 H), 3.73 (s, 2 H), 2.23 (s, 6 H); ^{13}C NMR δ 157.81 (s), 151.49 (d), 144.66 (s), 141.50 (s), 140.34 (s), 140.23 (s), 130.21 (d), 129.53 (d), 129.00 (s), 125.43 (d), 124.09 (d), 121.07 (s), 120.70 (d), 112.14 (d), 109.03 (s), 106.56 (d), 53.83 (t), 44.87 (q). Anal. ($C_{19}H_{18}BrN_5$) C, H, N.

5-[(3-Bromophenyl)amino]-3-[(4-morpholino)methyl]-pyrrolo[3,2-*g*]quinazoline (6) (37%): mp (EtOAc/petroleum ether) 229 °C dec; ^{1}H NMR [$(CD_3)_2SO$] δ 11.38 (s, 1 H), 9.82 (s, 1 H), 8.84 (s, 1 H), 8.52 (s, 1 H), 8.27 (t, J = 1.7 Hz, 1 H), 7.98 (d, J = 8.3 Hz, 1 H), 7.75 (s, 1 H), 7.61 (d, J = 2.1 Hz, 1 H), 7.37 (dd, J = 8.3, 8.3 Hz, 1 H), 7.29 (br d, J = 8.3 Hz, 1 H), 3.81 (s, 2 H), 3.59 (t, J = 4.4 Hz, 4 H), 2.48 (t, J = 4.4 Hz, 4 H); ^{13}C NMR δ 157.80 (s), 151.54 (d), 144.64 (s), 141.44 (s), 140.25 (s), 130.25 (d), 129.85 (d), 129.17 (s), 125.52 (d), 124.16 (d), 121.10 (s), 120.78 (d), 111.94 (d), 110.83 (s), 109.08 (s), 106.62 (d), 66.17 (t), 53.02 (t), 52.83 (t). Anal. ($C_{21}H_{20}BrN_5O$) C, H, N.

5-[(3-Bromophenyl)amino]-3-[[*N*,*N*-bis(2-hydroxyethyl)amino]methyl]pyrrolo[3,2-*g*]quinazoline (4). In this case the product was retained strongly on alumina, and purification was best achieved by chromatography on silica gel, eluting with MeOH/EtOAc (1:9) to give a yellow solid (18%): mp (EtOAc) 240−245 °C dec; ^{1}H NMR [$(CD_3)_2SO$] δ 11.30 (s, 1 H), 9.69 (s, 1 H), 8.84 (s, 1 H), 8.52 (s, 1 H), 8.30 (t, J = 1.9 Hz, 1 H), 7.97 (br d, J = 7.7 Hz, 1 H), 7.73 (s, 1 H), 7.63 (d, J = 1.9 Hz, 1 H), 7.37 (dd, J = 7.7, 7.6 Hz, 1 H), 7.29 (br d, J = 7.6 Hz, 1 H), 3.98 (s, 2 H), 3.53 (t, J = 6.0 Hz, 4 H), 2.65 (t, J = 6.0 Hz, 4 H); ^{13}C NMR δ 157.73 (s), 151.42 (d), 144.57 (s), 141.47 (s), 140.30 (s), 130.26 (d), 129.02 (d), 125.37 (d), 123.78 (d), 121.13 (s), 120.41 (d), 112.72 (s), 112.04 (d), 108.85 (s), 106.43 (d), 59.14 (t), 56.18 (t), 49.72 (t); FABMS found [M + H]$^+$ 458.1027, 456.1017, $C_{21}H_{23}BrN_5O_2$ requires 458.1015, 456.1035. Anal. ($C_{21}H_{23}BrN_5O_2$·H_2O) C, H.

5-[(3-Bromophenyl)amino]-3-[[*N*-(carboxymethyl)-*N*-methylamino]methyl]pyrrolo[3,2-*g*]quinazoline ethyl ester (8) (37%): mp (ETOAc/petroleum ether) 227−230 °C dec; ^{1}H NMR [$(CD_3)_2SO$] δ 11.35 (br s, 1 H), 9.78 (s, 1 H), 8.82 (s, 1 H), 8.53 (s, 1 H), 8.27 (br s, 1 H), 7.98 (d, J = 8.0 Hz, 1 H), 7.75 (s, 1 H), 7.59 (d, J = 2.0 Hz, 1 H), 7.37 (dd, J = 8.0, 8.0 Hz, 1 H), 7.28 (br d, J = 8.0 Hz, 1 H), 4.07 (q, J = 7.0 Hz, 2 H), 3.98 (s, 2 H), 3.34 (s, 3 H), 2.40 (s, 2 H), 1.16 (t, J = 7.0 Hz, 3 H); ^{13}C NMR δ 170.57 (s), 157.78 (s), 151.51 (d), 144.68 (s), 141.46 (s), 140.33 (s), 130.22 (d), 129.66 (d), 128.91 (s), 125.41 (d), 123.98 (d), 121.07 (s), 120.57 (d), 112.12 (d), 111.61 (s), 109.05 (s), 106.59 (d), 59.63 (t), 56.71 (t), 50.89 (t), 41.67 (q), 14.01 (q); DEIMS found M$^+$ 469.0917, 467.0929, $C_{22}H_{22}BrN_5O_2$ requires 469.0936, 467.0957.

A solution of the ester **8** (0.10 g, 0.22 mmol) in MeOH (10 mL) was stirred with 1 N NaOH (1 mL, 1.0 mmol) at room temperature for 1 h. Careful acidification with 1 N HCl gave 5-[(3-bromophenyl)amino]-3-[[*N*-(carboxymethyl)-*N*-methylamino]methyl]pyrrolo[3,2-*g*]quinazoline hydrochloride (**9**) (64 mg, 63%): mp (MeOH/Et_2O) 240 °C dec; ^{1}H NMR [$(CD_3)_2SO$] δ 12.41 (d, J = 1.9 Hz, 1 H), 11.91 (br, 1 H), 10.23 (s, 1 H), 8.97 (s, 1 H), 8.30 (dd, J = 1.9, 1.6 Hz, 1 H), 8.11 (d, J = 2.4 Hz, 1 H), 8.07 (s, 1 H), 8.05 (br d, J = 8.1 Hz, 1 H), 7.51 (dd, J = 8.2, 1.6 Hz, 1 H), 7.46 (dd, J = 8.2, 8.1 Hz, 1 H), 4.73 (s, 2 H), 4.21 (s, 2 H), 2.95 (s, 3 H); ^{13}C NMR δ 167.33 (s), 160.24 (s), 149.69 (d), 140.17, 138.92 (s), 135.57 (d), 130.46 (d), 129.85 (s), 128.54 (d), 126.59 (d), 123.09 (d), 121.08 (s), 119.47 (s), 116.19 (d), 107.50 (s), 103.87 (s), 100.21 (d), 53.90 (t), 50.21 (t), 39.91 (q); FABMS found [M + H]$^+$ 442.0685, 440.0734, $C_{20}H_{19}BrN_5O_2$ requires 442.0702, 440.0722.

Determination of Aqueous Solubility. Stock solutions of drugs were made up in methanol or DMSO and used to calibrate the HPLC (peak area in nanomoles, assuming a linear response). Accurately weighed amounts (to give approximately a 50 mM solution) were then sonicated for 30 min in 0.05 M sodium lactate buffer, pH 4.0 (neutral compounds, hydrochloride salts of amines), or in water (sodium salts of acids). After standing for an additional 30 min, the samples were centrifuged at 13 000 rpm for 3 min, and the concentration of drug in the supernatant was determined by HPLC, using the calibration determined previously.

Molecular Modeling. The 3D model of EGFR TK was constructed using the homology modeling module implemented in LOOK[25] with cAMP kinase as the template. The basis for the 3D model was the sequence alignment published recently by Knighton et al.[26] The EGFR TK inhibitors were constructed in SYBYL 6.2.[27] The charges for the small molecule inhibitors were derived from the semiempirical molecular orbital package MOPAC using the MNDO approach.[28] The inhibitors were docked manually into the ATP binding site, and geometry was optimized with the Tripos force field implemented in SYBYL 6.2 to relieve unfavorable steric contacts.

Enzyme Assay. Epidermal growth factor receptor was isolated from human A431 carcinoma cell shed membrane vesicles by immunoaffinity chromatography as previously described.[29] The enzyme assay was performed in 96-well filter plates (Millipore MADVN6550). The total volume was 0.1 mL containing 20 mM HEPES, pH 7.4, 50 μM sodium vanadate, 40 mM magnesium chloride, 10 μM ATP containing 0.5 μCi of [^{32}P]ATP, 20 μg of polyglutamic acid/tyrosine (Sigma Chemical Co., St. Louis, MO), 1 ng of EGFR tyrosine kinase, and appropriate dilutions of inhibitor. All components except the ATP were added to the well, and the plate was incubated with shaking for 10 min at 25 °C. The reaction was terminated by addition of 0.1 mL of 20% trichloroacetic acid (TCA) and the plate kept at 4 °C for at least 15 min to allow the substrate to precipitate. The wells were then washed five times with 0.125 mL of 10% TCA, and ^{32}P incorporation was determined with a Wallac beta plate counter. Control activity (no drug) gave a count of approximately 100 000 cpm. At least two independent dose−response curves were done and the IC_{50} values computed. The reported values are averages; variation was generally ±15%.

EGF Receptor Autophosphorylation in A431 Human Epidermoid Carcinoma Cells. Cells were grown to confluency in 6-well plates (35 mm diameter) and exposed to serum-free medium for 18 h. They were then treated with **8** for 2 h and with EGF (100 ng/mL) for 5 min. The monolayers were lyzed in 0.2 mL of boiling Laemlli buffer (2% sodium dodecyl sulfate, 5% β-mercaptoethanol, 10% glycerol, and 50 mM Tris, pH 6.8), and the lysates were heated to 100 °C for 5 min. Proteins in the lysate were separated by polyacrylamide gel electrophoresis and electrophoretically transferred to nitrocellulose. The membrane was washed once in 10 mM Tris, pH 7.2, 150 mM NaCl, and 0.01% azide (TNA) and blocked overnight in TNA containing 5% bovine serum albumin and 1% ovalbumin. The membrane was blotted for 2 h with antiphosphotyrosine antibody (UBI, 1 mg/mL in blocking buffer) and then washed twice in TNA, once in TNA containing 0.05% Tween-20 and 0.05% nonidet P-40, and twice in TNA. The membranes were then incubated for 2 h in blocking buffer containing 0.1 mCi/mL [^{125}I]protein A and then washed again as above. After the blots were dry they were loaded into a film cassette and exposed to X-AR X-ray film for 1−7 days. Band intensities were determined with a Molecular Dynamics laser densitometer.

Acknowledgment. This work was partially supported by the Auckland Division of the Cancer Society of New Zealand.

References

(1) El-Zayat, A. A. E.; Pingree, T. F.; Mock, P. M.; Clark, G. M.; Otto, R. A.; Von Hoff, D. D. Epidermal growth factor receptor amplification in head and neck cancer. *Cancer J.* **1991**, *4*, 375−380.

(2) Morishige, K.; Kurachi, H.; Amemiya, K.; Fujita, Y.; Yamamoto, T.; Miyake, A.; Tanizawa, O. Evidence for the involvement of transforming growth factor α and epidermal growth factor receptor autocrine growth mechanism in primary human ovarian cancers *in vitro*. *Cancer Res.* **1991**, *51*, 5322−5328.
(3) Jardines, L.; Weiss, M.; Fowble, B.; Greene, M. *Neu* (c-*erbB-2*/HER2) and the epidermal growth factor receptor (EGFR) in breast cancer. *Pathobiology* **1993**, *61*, 268−282.
(4) Hickey, K.; Grehan, D.; Reid, I. M.; O'Brian, S.; Walsh, T. N.; Hennessy, T. P. J. Expression of epidermal growth factor receptor and proliferating cell nuclear antigen predicts response of esophageal squamous cell carcinoma to chemoradiotherapy. *Cancer* **1994**, *74*, 1693−1698.
(5) Delarue, J. C.; Terrier, P.; Terrierlacombe, M. J.; Mouriesse, H.; Gotteland, M.; Maylevin, F. Combined overexpression of c-erbB-2 protein and epidermal growth factor receptor (EGF-r) could be predictive of early and long-term outcome in human breast cancer: a pilot study. *Bull. Cancer* **1994**, *81*, 1067−1077.
(6) Fry, D. W.; Kraker, A. J.; McMichael, A.; Ambroso, L. A.; Nelson, J. M.; Leopold, W. R.; Connors, R. W.; Bridges, A. J. A specific inhibitor of the epidermal growth factor receptor tyrosine kinase. *Science* **1994**, *265*, 1093−1095.
(7) Ward, W. H. J.; Cook, P. N.; Slater, A. M.; Davies, D. H.; Holdgate, G. A.; Green, L. R. Epidermal growth factor receptor tyrosine kinase. Investigation of catalytic mechanism, structure-based searching and discovery of a potent inhibitor. *Biochem. Pharmacol.* **1994**, *48*, 659−666.
(8) Rewcastle, G. W.; Denny, W. A.; Bridges, A. J.; Zhou, H.; Cody, D. R.; McMichael, A.; Fry, D. W. Tyrosine kinase inhibitors. 5. Synthesis and structure-activity relationships for 4-[(phenylmethyl)amino]- and 4-(phenylamino)quinazolines as potent adenosine-5′-triphosphate binding site inhibitors of the tyrosine kinase domain of the epidermal growth factor receptor. *J. Med. Chem.* **1995**, *38*, 3482−3487.
(9) Bridges, A. J.; Zhou, H.; Cody, D. R.; Rewcastle, G. W.; McMichael, A.; Showalter, H. D. H.; Fry, D. W.; Kraker, A. J.; Denny, W. A. Tyrosine kinase inhibitors. 8. An unusually steep structure activity relationship for analogues of 4-(3-bromoanilino)-6,7-dimethoxyquinazoline (PD 153035), a potent inhibitor of the epidermal growth factor receptor. *J. Med. Chem.* **1996**, *39*, 267−276.
(10) Rewcastle, G. W.; Palmer, B. D.; Bridges, A. J.; Showalter, H. D. H.; Nelson, J.; McPherson, A.; Kraker, A. J.; Fry, D. W.; Denny, W. A. Tyrosine kinase inhibitors. 9. Synthesis and evaluation of fused tricyclic quinazoline analogues as ATP site inhibitors of the tyrosine kinase activity of the epidermal growth factor receptor. *J. Med. Chem.* **1996**, *39*, 918−928.
(11) Rewcastle, G. W.; Palmer, B. D.; Thompson, A. M.; Bridges, A. J.; Fry, D. J.; Kraker, A. J.; Denny, W. A. Tyrosine kinase inhibitors. 10. Isomeric 4-[(3-bromophenyl)amino]pyrido[*d*]pyrimidines are potent ATP binding site inhibitors of the tyrosine kinase function of the epidermal growth factor receptor. *J. Med. Chem.* **1996**, *39*, 1823−1835.
(12) Barker, A. J. Tricyclic derivatives and their use as anti-cancer agents. Patent Application EPO 0 635 507 A1 to Zeneca Ltd., Jan. 21, 1995; *Chem. Abstr.* **1995**, *122*, 31545y.
(13) Himmelsbach, F.; von Ruden, T.; Dahmann, G.; Metz, T. Pyrimido[5,4-d]pyrimidines, drugs containing these compounds, their use, and process for preparing them. Patent Application PCT/EP95/03482 to Dr. Karl Thomae, GMBH, Sept. 5, 1995; *Chem. Abstr.* **1996**, *124*, 303748, 343326.
(14) Hudson, A. T.; Vile, S.; Barraclough, P.; Franzmann, K. W.; McKeown, S. C.; Page, M. J. Substituted heteroaromatic compounds and their use in medicine. Patent Application PCT/GB95/02202 to The Wellcome Foundation, Sept. 18, 1995; *Chem. Abstr.* **1996**, *125*, 114665.
(15) Showalter, H. D. H.; Sun, L.; Sercel, A. D.; Winters, R. T.; Denny, W. A.; Palmer, B. D. Concise syntheses of the novel 1*H*-pyrrolo[3,2-*g*]quinazoline ring system and its [2,3-*f*] angular isomer. *J. Org. Chem.* **1996**, *61*, 1155−1158.
(16) Thompson, A. M.; Bridges, A. J.; Fry, D. W.; Kraker, A. J.; Denny, W. A. Tyrosine kinase inhibitors. 7. 7-Amino-4-(phenylamino)- and 7-amino-4-[(phenylmethyl)amino]pyrido[4,3-d]pyrimidines; a new class of inhibitors of the tyrosine kinase activity of the epidermal growth factor receptor. *J. Med. Chem.* **1995**, *38*, 3780−3788.
(17) Zheng, J.; Trafny, E. A.; Knighton, D. R.; Xuong, N.-H.; Taylor, S. S.; Ten Eyck, L. F.; Sowadsky, J. M. 2.2 Å refined crystal structure of the catalytic subunit of cAMP-dependent protein kinase complexed with MnATP and a peptide inhibitor. *Acta Crystallogr.* **1993**, *D49*, 362−365.
(18) De Bondt, H. L.; Rosenblatt, J.; Jancarik, J.; Jones, H. D.; Morgan, D. O.; Kim, S. H. Crystal structure of cyclin-dependent kinase 2. *Nature* **1993**, *363*, 595−602.
(19) Zang, F.; Strand, A.; Robbins, D.; Cobb, M. H.; Goldsmith, E. J. Atomic structure of the MAP kinase ERK2 at 2.3 A resolution. *Nature* **1994**, *367*, 704−711.
(20) Owen, D. J.; Noble, M. E. M.; Garman, E. F.; Papageorgiou, A. C.; Johnson, L. N. Two structures of the catalytic domain of phosphorylase kinase: an active protein kinase complexed with substrate analogue and product. *Structure* **1995**, *3*, 467−482.
(21) Schulze-Gahmen, U.; Brandsen, J.; Jones, H. D.; Morgan, D. O.; Meijer, L.; Vesely, J.; Kim, S.-H. Multiple modes of ligand recognition: crysral structures of cyclin-dependent protein kinase 2 in complex with ATP and two inhibitors, olomucine and isopentyladenine. *Protein* **1995**, *22*, 378−391.
(22) Chen, H.; Bioziau, J.; Parker, F.; Maroun, R.; Tocque, B.; Roques, B.; Garbay-Jaureguiberry, C. Synthesis and structure-activity studies of a series of [(hydroxybenzyl)amino]salicylates as inhibitors of EGF receptor-associated tyrosione kinase activity. *J. Med. Chem.* **1993**, *36*, 4094−4098.
(23) Furet, P.; Caravatti, G.; Lydon, N.; Priestle, J. P.; Sowadski, J. M.; Trinks, U.; Traxler, P. Modelling study of protein kinase inhibitors - binding mode of staurosporine and origin of the selectivity of CGP 52411. *J. Comput.-Aided Mol. Des.* **1995**, *9*, 465−472.
(24) Traxler, P. M.; Furet, P.; Mett, H.; Buchdunger, E.; Meyer, T.; Lydon, N. 4-(Phenylamino)pyrrolopyrimidines: potent and selective, ATP site directed inhibitors of the EGF-receptor protein tyrosine kinase. *J. Med. Chem.* **1996**, *39*, 2285−2292.
(25) LOOK, Molecular Applications Group, Suite T, 445 Sherman Ave, Palo Alto, CA 94306.
(26) Knighton, D. R.; Cadena, D. L.; Zheng, J.; Ten Eyck, L. F.; Taylor, S. S.; Sowadski, J. M.; Gill, G. N. Structural features that specify tyrosine kinase activity deduced from homology modeling of the epidermal growth factor receptor. *Proc. Natl. Acad. Sci.* **1993**, *90*, 5001−5005.
(27) SYBYL molecular modeling software, Tripos E & S, 6548 Clayton Rd, St. Louis, MO 62117.
(28) Dewar, M. J. S.; Thiel, W. Ground states of molecules. 38. The MNDO method. Approximation and parameters. *J. Am. Chem. Soc.* **1977**, *99*, 4907.
(29) Gill, G. N.; Weber, W. Purification of functionally active epidermal growth factor receptor protein using a competitive antagonist monoclonal antibody and competitive elution with epidermal growth factor. *Methods Enzymol.* **1987**, *146*, 82−88.

JM960789H